Arch Pharm Res Vol 27, No 2, 265-272, 2004

Archives of Pharmacal Research
http://apr.psk.or.kr

Absorption, Distribution, Metabolism, and Excretion of CKD-732, a Novel Antiangiogenic Fumagillin Derivative, in Rats, Mice, and Dogs

Ho Sup Lee, Won Kyu Choi, Hoe Joo Son, Sung Sook Lee, Joon Kyum Kim, Soon Kil Ahn, Chung IL Hong, Hye-Ki Min[1], Myungsoo Kim[1], and Seung-Woon Myung[1]

Chong Kun Dang Research Institute, P.O. Box 74, Chonan 330-831, Korea and [1]Doping Control Center, Korea Institute of Science and Technology, P.O. Box 131, Seoul 136-791, Korea

(Received November 6, 2003)

The pharmacokinetics of CKD-732 (6-*O*-4-[dimethyl-aminoethoxy)cinnamoyl]-fumagillol · hemioxalate) was investigated in male SD rats and beagle dogs after bolus intravenous administration. The parent compound and metabolites obtained from *in vitro* and *in vivo* samples were determined by LC/MS. The main metabolite was isolated and identified as an *N*-oxide form of CKD-732 by NMR and LC/MS/MS. CKD-732 was metabolized into either **M11** or others by rapid hydroxylation, demethylation, and hydrolysis. The blood level following the intravenous route declined in first-order kinetics with $T_{1/2}\beta$ values of 0.72~0.78 h for CKD-732 and 0.92~1.09 h for **M11** in rats at a dose of 7.5~30 mg/kg. In dogs, $T_{1/2}\beta$ values of CKD-732 and **M11** were 1.54 and 1.79 h, respectively. Moreover, AUC values increased dose dependently for CKD-732 and **M11** in rats and dogs. The CLtot and Vdss did not change significantly with increasing dose, indicating linear pharmacokinetic patterns. The excretion patterns through the urine, bile, and feces were also examined in the animals. The total amount excreted in urine, bile, and feces was 2.13% for CKD-732 and 1.29% for **M11** in rats, and 1.58% for CKD-732 and 2.28% for **M11** in dogs.

Key words: CKD-732, Fumagillin derivative, Metabolism, Pharmacokinetics, HPLC/MS/MS

INTRODUCTION

Angiogenesis is a process of blood vessel development that occurs pathologically in diabetic retinopathy, scleroderma, psoriasis, fractures, arthritis, and inflammation. It is critical for the growth and regrowth of malignant solid tumors (Folkman, 1972, 1985, 1990; Folkman *et al.*, 1987). For these reasons, the discovery of antiangiogenic modulators was regarded as a promising area in cancer chemotherapy. Among them, fumagillin, a novel antibiotic secreted by *Aspergillus fumigatus fresnius*, exhibits potent antiangiogenic activity. However, fumagillin treatment is limited to clinical access because of its poor endothelial cell selectivity (Dipaolo *et al.*, 1958-1959; Ingber *et al.*, 1990; Killough *et al.*, 1952). The TNP-470 (6-*O*-(chloroacetylcarbamoyl)-fumagillol), a semisynthetic analogue of fumagillin developed by Takeda Chemical Co. (Japan), is 50 times more potent in inhibiting capillary growth with significantly reduced host toxicity. In spite of its potential for further development, TNP-470 displayed not only inadquate water solubility for enough pharmacological responses, but also poor pharmacokinetic properties with a very short half-life of around 10 minutes. In addition, it degraded to six metabolites in plasma (Ingber *et al.*, 1990; Kusaka *et al.*, 1991; Brem *et al.*, 1993), of which MIV (AGM-1883), an active metabolite, showed a plasma elimination half-life of less than 30 minutes. The metabolic pathway of TNP-470 involves extensive esterase cleavage, resulting in a more polar MII by epoxide hydrolase, followed by glucuronidation to MIII. The presence of MII and MIV in humans was recently reported (Placidi *et al.*, 1995, 1997, 1999; Cretton-Scott *et al.*, 1996).

Previously, we reported a novel synthetic fumagillin derivative, CKD-732 (6-*O*-[(4-dimethylaminoethoxy)cinnamoyl]-fumagillol hemioxalate) (Fig 1), which exhibited antitumor

Correspondence to: Seung-Woon Myung, Doping Control Center, Korea Institute of Science and Technology, P.O. Box 131, Seoul 136-791, Korea
Tel: 82-2-958-5104; Fax: 82-2-958-5059
E-mail: swmyung@kist.re.kr

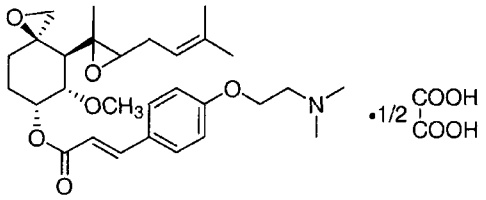

Fig. 1. Chemical structure of CKD-732, a novel antiangiogenic fumagillin derivative

and antimetastatic activities alone, while showing synergistic effect in combination with adriamycin, 5-FU, and cisplatin in an animal tumor model (Park *et al.*, 2001).

In the current study, we identified major metabolites of CKD-732 from *in vitro* and *in vivo* experiments and examined the metabolic patterns and pharmacokinetics, which were surprisingly different with those of TNP-470 despite their fumagillin moieties (Myung *et al.*, 2002).

EXPERIMENTAL

Chemicals

CKD-732 (6-*O*-[(4-dimethylaminoethoxy)cinnamoyl] fumagillol hemioxalate, 96.67%) was provided by a CKD research institute (Chonan, Korea). The drug was dissolved in 0.9% saline for injection. Nicotinamide-adenine dinucleotide phosphate (NADP), glucose-6-phosphate (G6P), glucose-6-phosphate dehydrogenase (G6PD), and potassium phosphate (KH_2PO_4) were purchased from Sigma Chemical Co., and heparin was a product of Shin Poong Pharm. Co. (Korea). Other chemicals were used as analytical or HPLC grade.

Animals

ICR mice (18~23 g) and male Sprague-Dawley (SD) rats (180~220 g) were purchased from Charles River Japan. Male beagle dogs (10~15 kg) were purchased from the Jackson Laboratory USA and were acclimated to laboratory conditions for 1 week prior to the start of the study. The animal room was maintained at 22±2°C and 60±5% relative humidity with a 12 h light/dark cycle. The animals were allowed free access to food and water, and were fasted overnight prior to drug administration.

HPLC analysis

Excretion studies were performed with a HPLC/UV-Vis system composed of a Waters 616 pump, Waters 996 Photodiode Array Detector. The HPLC/MS system for the metabolism, absorption and distribution was the Agilent 1100 Series LC/MSD Trap with electrospray ionization (ESI). The ESI conditions were a follows: positive ion polarity, 60 psi nebulizing gas pressure, 350°C drying gas temp., 10 L/min drying gas flow, and 80 eV capillary exit voltage. A Mightysil RP-18 column (250×4.6 mm, 5 um, Kanto Chemical Co., Japan) was used for the metabolism, absorption and distribution study, and a XTerra™MS C_{18} (2.1×150 mm, 5 um, Waters, USA) was used for the excretion study. A mixture of 20 mM ammonium acetate (pH 4.0, A) and acetonitrile (B) was used for the mobile phase. A gradient change of 30% to 70% of solvent B for 20 min with a flow rate of 1 mL/min was employed for the metabolism study. For the excretion study, acetonitrile (30%) was increased to 54% over 11 min, then increased to 80% over 13 min and finally held for 7 min at acetonitrile (80%) with a flow rate of 0.3 mL/min. The isocratic system (A : B = 50 : 50) was used for the absorption and distribution study with a flow rate of 1 mL/min at 306 nm.

Metabolism

Preparation of rat liver microsome

The rats were sacrificed by cervical dislocation. The livers were then removed after perfusion with saline and extensively washed with saline, after which they were cut into small pieces using scissors. The pieced were then homogenized with a Ultra-Turrax T25 homogenizer in 4 volumes of homogenizing buffer (100 mM Tris-acetate pH 7.4, 0.1 M KCl, 1 mM EDTA). The homogenate was centrifuged at 10,000 g for 20 min. The supernatant was carefully collected and ultracentrifuged at 105,000 g for 1 h using the Beckman Ultracentrifuge LA-80. Then the pellets were resuspended in homogenizing buffer and ultracentrifuged again at 105,000 g for 1 h. Afterwards, the liver microsomal pellets were resuspended in the suspension buffer (100 mM potassium phosphate buffer (pH 7.4), 20% (v/v) glycerol, 1 mM EDTA). After diluting the protein content to make 15~25 mg protein/mL, the liver microsome were stored at -70 °C

In vitro metabolism

The *in vitro* metabolism was performed at 37°C for 2 h in a NADPH-generating system of 0.5 mL incubation mixture containing 1 mg rat liver microsome, 100 uM CKD-732, 10 mM glucose-6-phosphate, 0.5 mg/mL NADP, glucose-6-phosphate dehydrogenase 1 unit, and 10 mM potassium phosphate buffer (pH 7.4). After incubation, the mixture was extracted with 2 mL methylene chloride, and the organic phase was dried under a stream of nitrogen. The residue was reconstituted in the mobile phase. Aliquots of 20 uL were injected onto HPLC/MS for metabolites identification.

In vivo metabolism

The plasma of the rats were collected at 10, 30, 60, and 240 min, the bile at 2, 4, and 6 h, and the urine at 24 h following intravenous administration of CKD-732 at a dose of 30 mg/kg. The collected plasma, urine, and bile were extracted with ethyl acetate and the organic phase was

evaporated in a vacuum. The residue was reconstituted with the HPLC mobile phase. Aliquots were injected into the HPLC/MS system.

Pharmacokinetics

Absorption

Polyethylene tube (PE-50, Nastume, Japan) was inserted into the carotid artery and the jugular vein of male SD rats under pentobarbital sodium (50 mg/kg, i.p.) anesthesia. CKD-732 was administered alone *via* the jugular vein cannular at a dose of 7.5, 15, and 30 mg/kg in rats, *via* the lateral tail vein at 30 mg/kg in male ICR mice, and *via* the cephalic vein at 5 mg/kg in beagle dogs. Blood samples were collected from all subjects at 5, 10, 30, 45, 60, 120, 180, 360, and 480 min after bolus intravenous dosing. All heparinized blood samples were immediately cooled in ice and centrifuged at 700 g (4°C) for 20 min. Plasma was stored at -70°C until HPLC analysis. Plasma protein was precipitated by the addition of 1 volume of CH_3CN and the aliquot (100 uL) of the supernatant, followed by vigorous agitation by vortex mixing and centrifuged again at 10,000 g for 10 min, was injected onto HPLC/UV-Vis.

Tissue distribution study

Female ICR mice were exsanguinated by heart puncture at 10, 30, 60, 120, 360, and 1440 min after intravenous administration of 30 mg/kg of CKD-732, and the collected blood was immediately centrifuged at 700 g (4°C) for 20 min. Plasma was separated by centrifugation at 700 g (4°C) for 20 min, and then stored at -70°C until HPLC/UV-Vis analysis. After exsanguinating the mice, the whole muscle, intestine, liver, lung, stomach, heart, spleen, ovary, thymus, and brain were quickly excised and washed with cold saline to eliminate the remaining blood. After blot drying with paper, the total weight of each tissue was measured, and each tissue was homogenized with 4

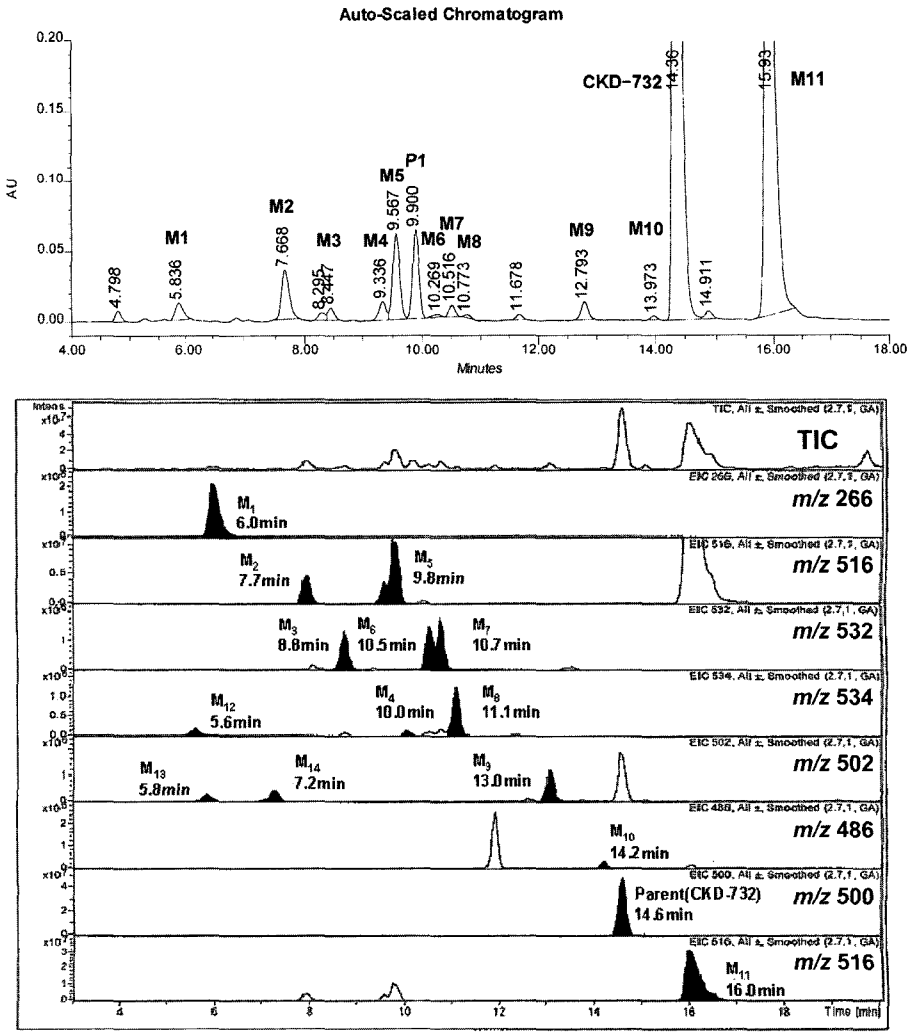

Fig. 2. Representative HPLC/UV-Vis (upper) and mass spectrometric (lower) chromatograms of *in vitro* microsomes from a male rat

volumes of 1.15% (w/v) KCl using a powergen homogenizer (Fisher Co., USA). After centrifugation, the supernatant was stored at -70°C until analysis.

Urinary, fecal and biliary excretion

The urine and feces samples were collected at 0, 8 (urine only), 24, 48, and 72 h after dosing 30 mg/kg of CKD-732 using a metabolic cage (Nalgene Co., USA) in bile-duct cannulated rats; bile samples were collected at 0, 2, 4, 6, 8, 24, 48, and 72 h after dosing. For analysis, 0.4 mL of bile and 1 mL of urine sample were extracted with 4 mL of ethylacetate and 3 mL of organic phase was evaporated in vacuum. The residue was reconstituted with 200 uL of the mobile phase. The feces samples were homogenized in 4-fold distilled water using a powergen homogenizer (Fisher Co, USA) and 1 mL of homogenate was treated as urine or bile. Their aliquots (20 uL) were injected onto HPLC/MS.

Pharmacokinetic analysis

The plasma concentration versus time data of CKD-732 for each subject in each regimen was analyzed by non-compartmental methods with the linear/log trapezoidal rule using WINNONLIN software (Scientific Consulting, Inc., USA).

Table I. Summary of chromatographic and MS data for CKD-732 metabolites from *in vitro* rat liver microsomal incubation, rat plasma, urine, and bile after bolus i.v. dosing of 30 mg/kg CKD-732

Metabolite	Molecular weight	RT[c] (min)	Percentage of total [b] (Mean peak area)			
			In vitro	Plasma	Urine	Bile
M1	265	6.0	0.95	-	-	-
BM1[a]	581	-	-	-	-	3.74
M2	515	9.4	2.74	-	1.87	1.88
UM1[a]	517	-	-	-	4.12	-
M3	531	8.8	0.56	-	-	6.63
M4	533	10.0	0.92	-	-	4.14
M5	515	9.8	4.18	-	4.56	1.82
M6	531	10.5	0.16	-	-	3.31
M7	531	10.7	0.52	-	-	9.27
M8	533	11.1	0.14	-	2.60	2.71
M9	501	13.0	0.93	-	-	-
PM1[a]	281	-	-	0.93	-	-
M10	484	14.2	0.16	-	7.33	0.99
CKD-732	499	14.3	46.18	68.09	51.28	13.63
BM2[a]	499	-	-	-	10.64	1.45
BM3[a]	547	-	-	-	-	2.09
M11	515	16.0	37.32	30.98	9.72	37.91
M12	533	5.6	<0.1	–	–	–
M13	501	5.8	<0.1	–	–	–
M14	501	7.2	<0.1	–	–	–
BM4[a]	515	–	–	–	–	6.46
UM2[a]	385	–	–	–	1.25	–

a) Unknown rat plasma (PM), urine (UM), and bile (BM) metabolites.
b) Mean extracted ion chromatogram peak area percent (>1%) of rat plasma (10, 30, 60, 240 min), urine (24 h), and bile (2, 4, 6 h) in MS spectrometry.
c) Retention time was calculated from *in vitro* rat microsomal metabolites.
– : Not determined

RESULTS

In vitro and *in vivo* metabolism study (Myung *et al.*, 2002)

The patterns of *in vitro* metabolites of CKD-732 after incubation with liver microsomes and *in vivo* plasma metabolites of rats are shown in Fig 2. The parent and fourteen metabolites were detected through microsomal incubation of CKD-732 and the main metabolite of CKD-732 was identified as the *N*-oxidation form of CKD-732 (M11). The chemical structure of **M11** was identified by NMR (Lee *et al.*, 2002), and the others were determined by HPLC/MS/MS spectrums and fragment ion analysis (Myung *et al.*, 2002). In contrast to the *in vitro* profiles, only one metabolite PM1 was found in rat plasma. In addition, **M11** was the major metabolite covering >30% of the mean total ion peak area (Fig 2, Table I).

Pharmacokinetic study

The plasma concentration versus time profiles of CKD-732 and **M11** following bolus intravenous administration of 5 mg/kg in beagle dogs are shown in Fig. 3. The mean plasma pharmacokinetic (PK) parameters for CKD-732 and **M11** in mice, rats and dogs were also obtained (Table

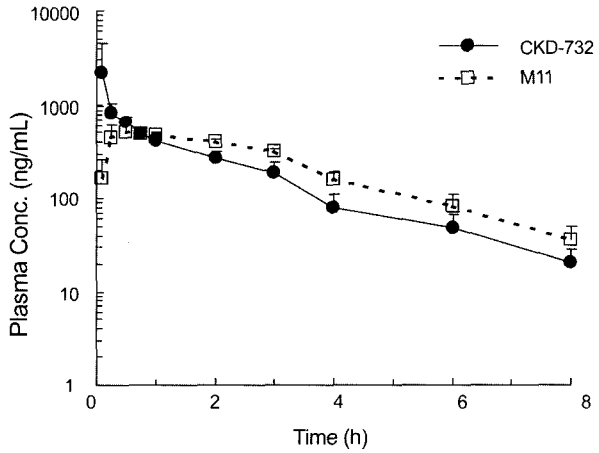

Fig. 3. Plasma concentration profiles of CKD-732 and **M11** after single bolus intravenous administration of 5 mg/kg CKD-732 in beagle dogs. Each point represents the mean±S.D. of 3 dogs. ●; CKD-732, □; **M11** (major metabolite of CKD-732).

Table II. Pharmacokinetic parameters of CKD-732 after intravenous administration in experimental animals (n=5)

Species	Compound	Dose (mg/kg)	Pharmacokinetic parameters					
			C_0[a] (ng/mL)	$T_{1/2}\beta$ (h)	$AUC_{0\to\infty}$ (ng·h/mL)	CLtot (L/h/kg)	Vdss (L/kg)	MRT (h)
Mouse[b]	CKD-732	30	3230.45	0.82	668.47	44.88	22.47	0.50
	M11		218.40	0.64	142.41	210.66	171.57	0.81
Rat	CKD-732	7.5	344.34 ± 118.53	0.72 ± 0.16	213.40 ± 63.08	35.14 ± 8.91	30.26 ± 6.59	0.86 ± 0.14
	M11		188.87 ± 51.04	1.04 ± 0.22	293.34 ± 89.10	25.57 ± 7.91	40.95 ± 20.77	1.66 ± 0.39
	CKD-732	15	517.26 ± 205.48	0.76 ± 0.11	442.77 ± 82.22	35.34 ± 6.41	38.64 ± 8.53	1.06 ± 0.19
	M11		376.71 ± 204.83	0.92 ± 0.13	467.05 ± 55.77	31.58 ± 4.15	45.11 ± 8.77	1.41 ± 0.22
	CKD-732	30	1227.22 ± 239.19	0.78 ± 0.13	812.98 ± 95.01	37.23 ± 4.71	35.57 ± 7.07	1.01 ± 0.22
	M11		712.36 ± 113.96	1.09 ± 0.12	1069.86 ± 171.96	27.70 ± 3.98	45.53 ± 9.98	1.72 ± 0.23
Dog[c]	CKD-732	5	1170.63 ± 434.03	1.54 ± 0.13	1619.19 ± 339.72	3.09 ± 0.62	6.25 ± 0.96	2.02 ± 0.29
	M11		529.54 ± 91.98	1.79 ± 0.21	1889.09 ± 164.93	2.65 ± 0.23	7.58 ± 0.82	2.89 ± 0.44

a) Initial concentration
b) Pharmacokinetic parameters were estimated from the mean plasma concentration of five mice pooled.
c) N= 3

II). Furthermore, the plasma concentration of CKD-732 after single bolus intravenous administration in the rats, mice, and dogs are shown Fig. 4. The plasma concentration-time profiles of CKD-732 declined to a weak bi-exponential phase and rapidly metabolized to **M11** *in vivo* after dosing.

Tissue distribution study

The mean concentrations of CKD-732 in the tissues of female mice following a single intravenous dose of 30 mg/kg are listed in Table III. CKD-732 and **M11** were not detected from 6 h after administration in almost every organ tissue, and their elimination half-lives were below 1 h.

Excretion study

After intravenously administering 15 mg/kg of CKD-732 in bile duct-cannulated rats, the urinary, biliary, and fecal excretions were examined for 72 h using a metabolic cage (Table IV). The excretion profiles showed that CKD-732 and **M11** were mainly excreted by 8 h in amounts that were negligible compared to the total administered dose.

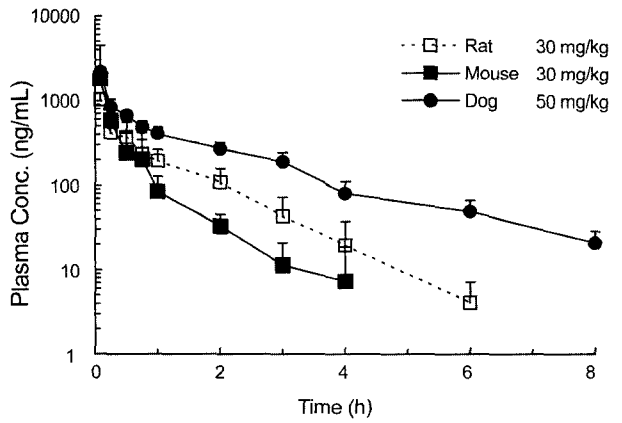

Fig. 4. Plasma concentration profiles of CKD-732 after single bolus intravenous administration in experimental animals. Each point represents the mean±S.D. ■ ; mouse (30 mg/kg, n=5), □; rats (30 mg/kg, n=5), ●; dogs (5 mg/kg, n=3).

DISCUSSION

The structures of fourteen metabolites identified by LC/MS/MS are shown in Fig 5. The metabolic ratios were determined by the extracted ion peak ratio because of the extremely low urinary and biliary excretion rates at the administered doses. The parent drug (CKD-732) and major metabolites identified by LC/MS/MS were assayed in the rats and dogs, and their pharmacokinetics indicated high clearance. After bolus intravenous administration, CKD-732 was metabolized and over 20 metabolite peaks in urine and bile were detected. Among them, nine metabolites from the urine and fourteen from the bile sample covered >1% of total ion peak area, and the metabolic patterns were almost identical to those of the metabolites *in vitro* (Table I). It is likely that the major metabolic pathway of CKD-732 was closely associated with the *N*-oxidation process, and the main metabolite in bile and plasma was **M11**, but not in urine (Table I). The means of conjugation remains to be further investigated. The major active metabolite, **M11**, was pharmacologically active and its plasma concentration level was comparable to the parent drug, with 5~10 times more potent activity in the endothelial cell growth than fumagillin (Lee *et al.*, 2002). The LOQ (limit of quantitation, S/N=6) and LOD (limit of detection, S/N=2) of CKD-732 in plasma analyzed by HPLC/UV-Vis were 9.90 and 3.27 ng/mL, respectively, and,

Table III. Tissue concentrations of CKD-732 (A) and **M11** (B) after single bolus intravenous administration at a dose of 30 mg/kg CKD-732 in female ICR mice

(A)

Tissue	Time after administration					
	10 min	30 min	1 h	2 h	6 h	24 h
Plasma	2.821 ± 0.468	1.123 ± 0.243	0.399 ± 0.080	0.171 ± 0.054	–	
Brain	9.239 ± 1.423	3.589 ± 0.519	1.172 ± 0.232	0.352 ± 0.110	–	
Heart	12.643 ± 1.427	5.447 ± 1.378	1.922 ± 0.418	0.902 ± 0.452	–	
Liver	6.979 ± 0.767	2.564 ± 0.157	1.233 ± 0.305	0.716 ± 0.352	–	
Lung	40.703 ± 8.792	22.484 ± 4.278	7.859 ± 2.702	3.470 ± 1.499	–	
Kidney	0.541 ± 0.223	0.590 ± 0.405	0.212 ± 0.104	0.106 ± 0.127	–	
Spleen	15.483 ± 3.122	10.221 ± 1.956	3.461 ± 0.848	1.460 ± 0.698	–	
Stomach	8.245 ± 2.611	3.842 ± 2.200	4.128 ± 3.782	1.856 ± 0.970	0.023 ± 0.052	
Thymus	9.370 ± 1.451	6.019 ± 0.984	3.431 ± 0.291	1.509 ± 0.599	–	
Intestine	2.230 ± 0.979	1.192 ± 0.270	0.914 ± 0.210	0.593 ± 0.203	–	
Muscle	4.681 ± 1.592	2.567 ± 1.142	0.837 ± 0.361	0.274 ± 0.179	–	
Ovary	11.031 ± ?.636	9.861 ± 2.124	5.236 ± 1.584	2.765 ± 0.762	–	-

(B)

Tissue	Time after administration					
	10 min	30 min	1 h	2 h	6 h	24 h
Plasma	0.408 ± 0.068	0.252 ± 0.062	0.072 ± 0.027	0.025 ± 0.006	–	–
Brain	0.088 ± 0.016	0.100 ± 0.002	0.033 ± 0.011	0.033 ± 0.007	–	–
Heart	0.295 ± 0.049	0.304 ± 0.070	0.118 ± 0.025	0.189 ± 0.033	–	–
Liver	0.757 ± 0.122	0.411 ± 0.080	0.207 ± 0.223	0.379 ± 0.163	–	–
Lung	2.689 ± 0.640	1.215 ± 0.216	0.541 ± 0.180	0.284 ± 0.124	–	–
Kidney	0.586 ± 0.185	0.721 ± 0.042	0.299 ± 0.075	0.365 ± 0.111	–	–
Spleen	0.237 ± 0.079	0.567 ± 0.053	0.224 ± 0.027	0.282 ± 0.038	–	–
Stomach	1.459 ± 0.773	1.278 ± 0.603	1.794 ± 1.103	2.776 ± 0.523	0.273 ± 0.224	–
Thymus	0.209 ± 0.080	0.263 ± 0.033	0.158 ± 0.020	0.236 ± 0.056	–	–
Intestine	0.243 ± 0.143	0.311 ± 0.112	0.395 ± 0.115	0.495 ± 0.139	–	–
Muscle	0.083 ± 0.035	0.128 ± 0.054	0.040 ± 0.014	0.044 ± 0.034	–	–
Ovary	0.198 ± 0.140	0.536 ± 0.143	0.371 ± 0.112	0.465 ± 0.092	–	–

– : not detected

Table IV. Urinary, biliary and fecal excretion of CKD-732 after intravenous administration of 15 mg/kg in bile duct-cannulated rats

	Time (h)	Excretion (%)		Total
		CKD-732	M11	
Urine	0~8	1.20 ± 0.31	0.48 ± 0.24	1.68 ± 0.44
	8~24	0.19 ± 0.05	0.19 ± 0.09	0.39 ± 0.11
	24~48	0.09 ± 0.04	0.01 ± 0.01	0.11 ± 0.05
	48~72	0.02 ± 0.01	0.00 ± 0.00	0.02 ± 0.01
	Total	1.51 ± 0.31	0.68 ± 0.21	2.19 ± 0.41
Feces	0~24	0.018 ± 0.008	0.003 ± 0.004	0.021 ± 0.010
	24~48	0.002 ± 0.004	–	0.002 ± 0.004
	48~72	–	–	–
	Total	0.020 ± 0.010	0.003 ± 0.004	0.023 ± 0.013
Bile	2	0.37 ± 0.24	0.45 ± 0.07	0.82 ± 0.27
	4	0.17 ± 0.09	0.13 ± 0.06	0.30 ± 0.10
	6	0.04 ± 0.03	0.02 ± 0.01	0.06 ± 0.04
	8	0.01 ± 0.01	–	0.01 ± 0.01
	24	0.01 ± 0.01	–	0.01 ± 0.01
	48	–	–	–
	72	–	–	–
	Total	0.60 ± 0.28	0.61 ± 0.10	1.20 ± 0.29
Total		2.13 ± 0.31	1.29 ± 0.25	3.42 ± 0.43

– : not detected

in contrast to TNP-470, CKD-732 was stable at the neutral pH (data not shown). Consequently, the metabolic pattern and pathway of CKD-732 were found to be clearly different from those of TNP-470 in view of the existence of the aromatic moiety in CKD-732, not present in TNP-470, which might provide relatively better protection of the active site of epoxide in the fumagillin moiety from metabolic enzyme.

CKD-732 and **M11** exhibited similar plasma concentration levels and could be detected until 6~8 h after administration in the rats and dogs (Fig. 3).

From the pharmacokinetic parameters of CKD-732 and **M11** shown in Table II, at the CKD-732 dose levels of 7.5, 15, and 30 mg/kg in the rats, the Cmaxs were 344.3, 517.3 and 1227.2 ng/mL, and for **M11** they were 188.9, 376.7 and 712.4 ng/mL. The AUC values increased dose-dependently with 213.4, 442.8 and 813.0 ng·h/mL for CKD-732, and 293.4, 467.1 and 1069.9 ng·h/mL for **M11**. The apparent elimination half-life values ($T_{1/2}\beta$) of 0.72~0.78 h for CKD-732 and 0.92~1.09 h for **M11** were observed. Of which $T_{1/2}\beta$, CLtot and Vdss showed no significant difference with dose escalation. In the beagle dogs, the apparent elimination half-life values of CKD-732 and

M11 were 1.54 h and 1.79 h, respectively, after 5 mg/kg CKD-732; the Cmax, $AUC_{0\rightarrow\infty}$, CLtot and Vdss were 1170.63 ng/mL, 1619.19 ng·h/mL, 3.09 L/h/kg, 6.25 L/kg for CKD-732 and 529.54 ng/mL, 1889.09 ng·h/ml, 2.65 L/h/kg, 7.58 L/kg for **M11**. After bolus intravenous dosing of 30 mg/kg CKD-732 in mice, the AUC values were 668.47 ng·h/mL for CKD-732 and 218.4 ng·h/mL for **M11**, and CLtot values were 44.88 L/h/kg for CKD-732 and 210.66 L/h/kg for **M11**. Meanwhile, the AUC value of **M11** in mice was relatively lower than that in rats, which was considered to be due to the different **M11** metabolizing rates between mice and rats. Based on these results, it can be said that CKD-732 is expected to be a more promising antitumor agent requiring a long half-life in plasma.

From the tissue concentration of CKD-732 and **M11** in ICR mice (Table III), the $AUC_{0\rightarrow24h}$ of CKD-732 posted the highest values in the lung, followed, in descending order, by the ovary, spleen, stomach, thymus, heart, brain, liver, and plasma. The CKD-732 and **M11** were also rapidly eliminated from tissue organs like those of plasma in mice. Therefore, there was no possibility of accumulation in the tissue organ with daily dosing.

As shown the urinary, biliary and fecal excretion data of the bile duct-cannulated rats (Table IV), the recovery percentages of CKD-732 and **M11** excreted into urine, bile, and feces were 2.19±0.41%, 0.023±0.013 and 1.2±0.29%,

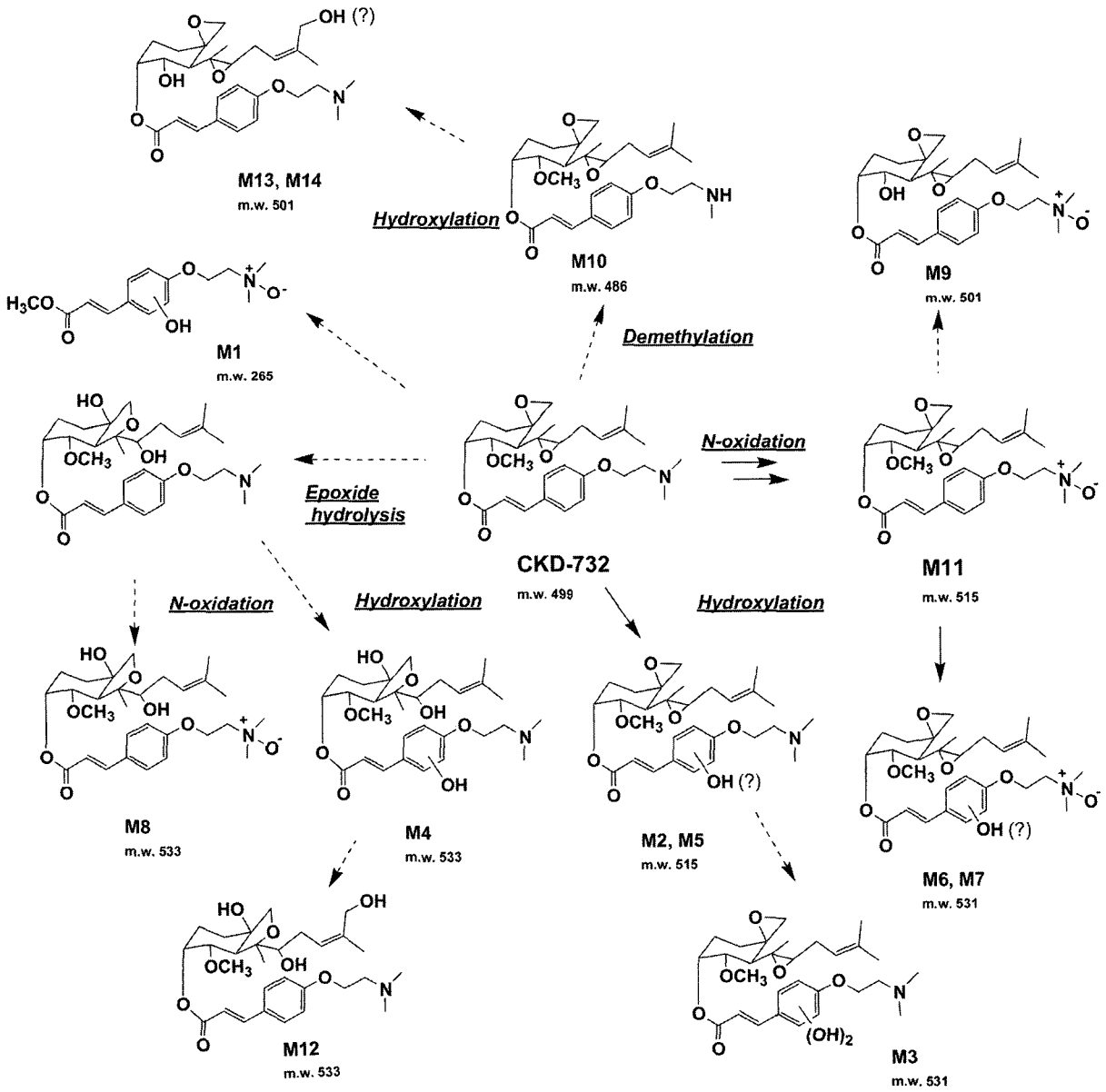

Fig. 5. Proposed metabolic pathway of *in vitro* rat microsomal metabolites of CKD-732

respectively. Among them, the total percentage excreted into urine, bile, and feces were 2.13±0.31% with CKD-732 and 1.29±0.25% with **M11**, resulting in the excretion of 3.42±0.434% of the total administered dose. The excretion profiles showed that CKD-732 and **M11** were mainly excreted by 8 h in amounts that were negligible compared to the total administered dose. Meanwhile, similar findings were obtained from the beagle dogs: by 96 h, CKD-732 and **M11** were excreted into urine at the rates of 0.45% and 0.61%, respectively, and into feces at the rates of 1.13% and 0.08% of the total administered dose, respectively (data not shown). From the results above, CKD-732 metabolized extensively before its elimination, which corresponds to the findings showing that CKD-732 and **M11** disappeared at 6 h after dosing in almost every tissue organ.

CONCLUSION

The tissue concentration levels of CKD-732 and **M11** were highest in lung, followed in descending order, by the heart, spleen and ovary, but both of them were not detected from 6 h after administration in all organ tissues of ICR mice. These results indicated that CKD-732 has a relatively improved metabolic pattern with around 40 min of $T_{1/2}\beta$ for both parent and major metabolites, compared to those of other fumagillin derivatives.

REFERENCES

Brem, H. and Folkman, J., Analysis of experimental anti-angiogenic therapy. *J. Pediatr. Surg.*, 28, 445-450; Discussion 450-451 (1993).

Cretton-Scott, E., Placidi, L., McClure, H., Anderson, C. D., and Sommadossi, J. P., Pharmacokinetics and metabolism of *O*-(chloroacetyl-carbamoyl) fumagillol (TNP-470, AGM-1470) in rhesus monkeys. *Cancer Chemother. Pharmacol.*, 38, 117-122 (1996).

Dipaolo, J., Tarbell, D., and Moore G., Studies on the carcinolytic activity of fumagillin and some of its derivatives. *Antibiot. Annu.*, 541-546 (1958-1959).

Folkman, J. and Klagsbrun, M., Angiogenic factors. *Science*, 235, 442-447 (1987).

Folkman, J., Tumor angiogenesis. *Adv. Cancer Res.*, 43, 175-203 (1985).

Folkman, J., Anti-angiogenesis: new concept for therapy of solid tumors. *Ann. Surg.*, 175, 409-416 (1972).

Folkman, J., What is the evidence that tumors are angiogenesis dependent? *J. Natl. Cancer Inst.*, 82, 4-6 (1990).

Ingber, D., Fujita, T., Kishimoto, S., Sudo, K., Kanamaru, T., Brem, H., and Folkman, Synthetic analogues of fumagillin that inhibit angiogenesis and suppress tumour growth. *Nature*, 348, 555-557 (1990).

Killough, J., Magill, G., and Smith, R., The treatment of amoebiasis with fumagillin. *Science*,115, 71-72 (1952).

Kusaka, M., Sudo, K., Fujita, T., Marui, S., Itoh, F., Ingber, D., and Folkman, J., Potent anti-angiogenic action of AGM-1470: comparison to the fumagillin parent. *Biochem. Biophys. Res. Commun.*, 174, 1070-1076 (1991).

Lee, H. S., Kim, H. Y., Sohn, Y. S., Choi, W. K., Son, H. J., Lee, S. S., Myung, S.-W., Kim, J. K., Ahn, S. K., and Hong, C. I., Metabolism and Pharmacokinetic study of CKD-732. *American Association for Cancer Research (93rd AACR)*, 43, 181 (2002).

Myung, S. W., Kim, H. Y., Min, H. K., Kim, D. H., Kim, M. S., Cho, H., W., Lee, H. S., Kim, J. K., and Hong, C. I., The identification of *in vitro* metabolites of CKD-732 by liquid chromatography/tandem mass spectrometry. *Rapid Commun. Mass Spectrom.*, 16, 2048-2053 (2002).

Park, H. J., Shon, Y. S., Son, H. J., Moon, S. K., Kim, J. G., Kim, J. K., Ahn, S. K., and Hong, C. I., Combination chemotherapy and preliminary toxicity of CKD-732, a novel fumagillin derivative. *American Association for Cancer Research (92nd AACR)*, 42, 87 (2001).

Placidi, L., Cretton-Scott, E., De Sousa, G., Rahmani, R., Placidi, M., and Sommadossi, J. P., Disposition and metabolism of the angiogenic moderator *O*-(chloroacetylcarbamoyl) fumagillol (TNP-470, AGM-1470) in human hepatocytes and tissue micorosomes. *Cancer Res.*, 55, 3036-3042 (1995).

Placidi, L., Cretton-Scott, E., De Sousa, G., Rahmani, R., Placidi, M. and Sommadossi, J. P., Interspecies variability of TNP-470 metabolism, using primary monkey, rat and dog cultured hepatocytes. *Drug Metab. Dispos.*, 25, 94-99 (1997).

Placidi, L., Cretton-Scott, E., Eckoff, D., Bynon, S., and Sommadossi, J. P., Metabolic drug interactions between angiogenic inhibitor, TNP-470 and anticancer agents in primary cultured hepatocytes and microsomes, *Drug Metab. Dispos.*, 27, 623-626 (1999).